Modeling and Analysis of Distribution Power System at UFLA Using OpenDSS

Sílvia Costa Ferreira, Ronnielli Chagas de Oliveira, Alexandre de Araújo, Alexandre Luiz da Silva, Marcelo Arriel Rezende, João Paulo de Carvalho Pedroso, and Joaquim Paulo da Silva

***Abstract*—The increasing integration of Distributed Energy Resources (DERs) in power distribution networks demands accurate system modeling and reliable power flow analysis. This paper presents a structured methodology for modeling a real Electrical Distribution System (EDS) using OpenDSS, applied to the Federal University of Lavras (UFLA), Brazil. Due to the lack of georeferenced data, the method combines satellite-based geolocation with load characterization from real measurements and statistical distributions. The model supports deterministic and time-series power flow simulations under three conditions: without DERs, with a 1.2 MWp photovoltaic plant, and with additional power factor correction. To achieve this, an incremental algorithm is proposed to determine the optimal size of a fixed capacitor bank at the feeder, improving the power factor without violating constraints. Results showed that DER integration reverses power flow, increases losses, and reduces the power factor, which also becomes variable and highly dependent on photovoltaic generation, but is improved by the proposed algorithm. This methodology enables effective, simplified modeling and analysis of real-world EDSs.**

Link to graphical and video abstracts, and to code: https://latamt.ieeer9.org/index.php/transactions/article/view/9769

***Index Terms*—Capacitor Bank Sizing, Deterministic Power Flow Analysis, Distribution System Planning.**

I. Introduction

In recent years, Electrical Distribution Systems (EDS) have experienced a significant paradigm shift, driven by the increasing integration of Distributed Energy Resources (DERs) and growing demand for enhanced system flexibility and resilience [1], [2]. The incorporation of DERs has prompted novel methodologies for effective planning, optimized operation, and advanced control strategies within EDSs [3], [4].

To properly address this evolving landscape, several studies have been conducted, primarily focusing on loss reduction, energy efficiency improvement, and the optimal integration of diverse resources. Among the most prominent methodologies in the literature are topology reconfiguration [5], hosting capacity analysis [6]–[9], and the optimal placement of capacitor banks [10], distributed generation units [11], energy storage systems [12], and electric vehicle infrastructure [13].

The associate editor coordinating the review of this manuscript and approving it for publication was Gabriel Pinto (*Corresponding author: Silvia Costa Ferreira*).

Silvia Costa Ferreira, R. C. de Oliveira, A. de Araújo, A. L. da Silva, M. A. Rezende, J. P. de C. Pedroso, and J. P. da Silva are with the Federal University of Lavras, Lavras, MG, Brazil (e-mails: silvia.ferreira@ufla.br, ronnielli.oliveira@gmail.com, alexandreajac@hotmail.com, alexandre.silva@ufla.br, marceloarriel@gmail.com, pedroso.jpc@gmail.com, and joaquim@ufla.br).

These approaches inherently rely on power flow simulations to evaluate system performance under steady-state or time-varying conditions [14]. However, when applied to real-world EDSs, such analyses demand accurate and detailed models of both primary and secondary networks that reflect the actual configuration and operational characteristics. Acquiring such detailed data is challenging due to the reliance on costly and time-consuming field surveys, as well as the frequent incompleteness or obsolescence of available data [15].

To overcome these limitations, recent studies have explored automated strategies for converting utility data into OpenDSS-compatible models. In [16], a Python-based tool was used to transform non-standard utility data into simulation-ready formats, while [17] proposed a plugin that generates OpenDSS models directly from QGIS georeferenced data. Although both approaches were validated with real measurements, they offer limited detail on spatial modeling and secondary networks.

A more detailed approach is presented in [18], where a high-fidelity model was built by converting a CYME database into OpenDSS using a custom tool. Loads and PV units were defined from actual measurements, and GIS data supported asset geolocation. The study also developed time-series profiles for demand and generation, demonstrating that detailed modeling of secondary feeders significantly improves simulation accuracy when compared to field data.

Despite recent advances, the literature still lacks methodologies for modeling real EDSs in OpenDSS when georeferenced data, GIS information, or commercial software outputs are unavailable. Building such models from scratch remains time-consuming and costly [19]. To address this gap, this paper proposes a structured and lightweight methodology for modeling real EDSs directly within the OpenDSS environment. The proposed approach leverages satellite imagery from Google Maps to extract the geographic coordinates of poles, transformers, loads, and DER units, which are used to accurately represent the spatial layout of both primary and secondary circuits. These spatial data are complemented by nameplate information from transformers and conductor specifications for both primary and secondary feeders, collected through field inspections. This process reduces the volume of data required from fieldwork, minimizes data acquisition time, and eliminates the need for intermediary steps involving data conversion between software platforms.

This methodology is applied to the modeling of the Electrical Distribution System (EDS) of the Federal University of Lavras (UFLA), located in Minas Gerais, Brazil. The system consists of a medium-voltage radial network with multiple

Distributed Energy Resource (DER) connections, including a 1.2 MWp photovoltaic system. The model is developed in OpenDSS and evaluated through both deterministic and time-series (24-hour) simulations across three operating scenarios: (i) without DERs, (ii) with DERs connected, and (iii) with DERs and reactive power compensation using fixed capacitor banks. Additionally, a simple yet effective algorithm is implemented to determine the optimal size of fixed capacitor banks. This deterministic incremental approach enhances the modeling framework by offering a practical method for systems whose power factor varies throughout the day and strongly depends on the photovoltaic generation profile.

Given the compact size and institutional nature of the studied network, where electrical loads are concentrated in relatively spaced buildings, this modeling approach proves both feasible and efficient, as it simplifies the overall workflow. The main contributions of this paper are as follows:

- A concise methodology for modeling real EDSs via satellite imagery (Google Maps), reducing fieldwork and enabling OpenDSS simulations without preexisting data;
- Application to the UFLA distribution network, covering system topology, load allocation, and DER integration in a compact institutional system;
- Development of a deterministic incremental algorithm to determine the optimal size of fixed capacitor banks, supporting reactive power compensation.

II. Methodology for Modeling the UFLA EDS

The modeling of the UFLA Electrical Distribution System (EDS) followed a structured procedure divided into two phases. Phase I encompasses data collection and field surveys, whereas Phase II involves load modeling and power flow analysis using OpenDSS. Phase I, focused on system characterization and data acquisition, includes the steps:

(a) **Characterization of the EDS and feeder:** General operational data, maintenance procedures, and protection schemes of the EDS are collected. The feeder is modeled considering its nominal voltage level and short-circuit current;
(b) **Geographical coordinates of poles, transformers, and secondary circuits:** Poles, transformers, and secondary circuits for each building are georeferenced using *Google Maps*. Distances and positions (latitude and longitude) are obtained from satellite imagery. Secondary circuits are traced based on the visible campus layout;
(c) **Transformer characteristics:** On-site photographs of transformer nameplates are captured to gather relevant specifications such as rated power, nominal voltage, connection type, and percent impedance;
(d) **Cable characteristics per segment:** Detailed data on cables used in each segment are collected, including cross-sectional areas and manufacturer specifications;
(e) **Characterization of photovoltaic installations:** Existing photovoltaic systems within the defined study area are surveyed, including details of maximum generation capacity, grid connection points, and associated cabling;
(f) **Photovoltaic generation curve:** Empirical data representative of typical photovoltaic generation profiles, analogous to the characteristics of the UFLA PV plant, are collected and analyzed;
(g) **Demand profiles:** UFLA's demand curves are analyzed by processing data from the main feeder, covering the period from July 1, 2022, to August 31, 2023. This analysis aims to identify maximum and minimum demand levels recorded and establish a representative daily profile.

Subsequently, Phase II, which comprises load modeling and computational studies using OpenDSS software, is executed following the steps outlined below:

(a) **Distribution of loads across transformers:** Loads are assigned to each transformer based on a normal distribution, aligning with the average load under maximum and minimum demand. This ensures a representative load profile and statistical consistency in the system model;
(b) **Studies using OpenDSS:** Collected data are integrated into the UFLA distribution system model in OpenDSS. Deterministic and daily time-series power flow analyses evaluate the EDS model's performance and quantify photovoltaic generation impacts.

The behavior of certain components, such as fuses and sectionalizing switches, is not addressed in the present study and may be incorporated into future research efforts. Moreover, the proposed methodology presents flexibility and can be extended to facilitate the modeling of other real-world EDSs.

III. Data Collection Procedure

The UFLA EDS was modeled using the data described in Section II, which is presented and discussed below.

A. Characteristics of the Electrical Distribution System

The campus EDS at UFLA is managed by the university's internal technical staff, operating in compliance with established protection and operational standards. The campus is supplied by a dedicated medium-voltage feeder, equipped with a 15 kV circuit breaker and overcurrent protection managed by a SEG MR11 relay, which does not have remote communication capabilities. At the point of common coupling, the feeder presents short-circuit current levels of 1063 A (single-phase-to-ground) and 3188 A (three-phase) at 13.8 kV. The institution's total contract demand is 2600 kW.

The network operates at a nominal line-to-line voltage of 13.8 kV, with medium-voltage distribution delivered via overhead lines. Step-down transformers, configured in Dyn1 connection, reduce the line-to-line voltage to 220 V, with low-voltage distribution predominantly carried out through underground cables. Responsibility for the internal distribution network lies exclusively with the university, rather than with the local electric utility provider.

B. Georeferenced Coordinates of Distribution Poles

The geographic coordinates of the poles were surveyed using *Google Maps* [20]. Fig. 1a illustrates the modeled area, in which the points depicted on the map correspond to

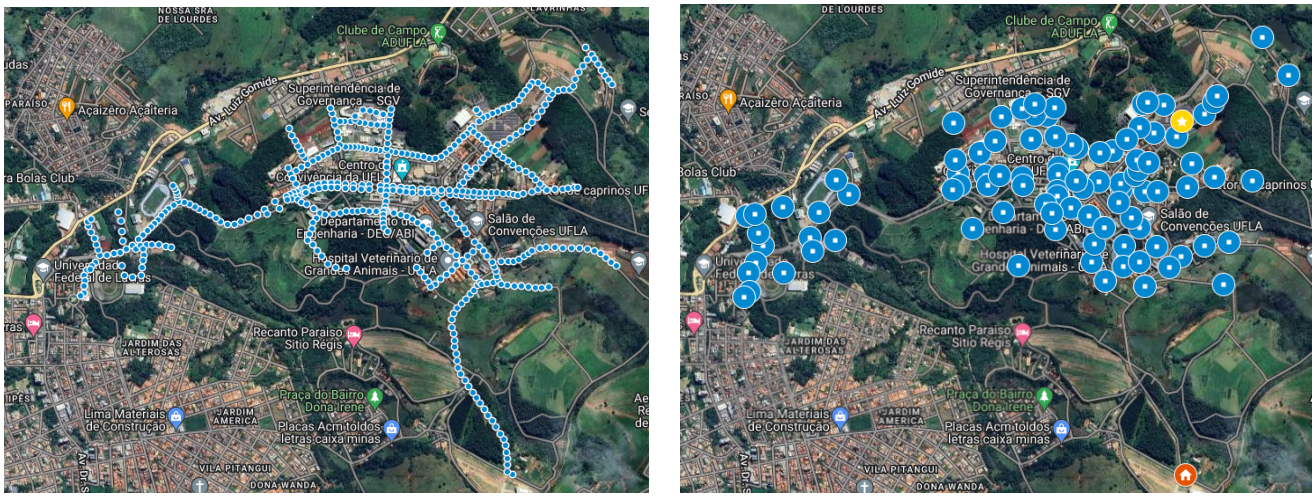

(a) Poles (b) Transformers

Fig. 1. Representation of pole and transformer locations using *Google Maps* (a) Poles (b) Transformers [20].

each surveyed pole, precisely georeferenced by latitude and longitude. In total, 460 poles were identified, along with their respective geographic coordinates and inter-pole distances, resulting in approximately 17.69 km of surveyed infrastructure.

C. Transformer Specifications

The transformer power ratings (kVA) and series impedance ($z\%$) values are surveyed from on-site photographic records of transformer nameplates. In a few cases, the nameplates presented illegible or incomplete information. In such instances, the impedance values ($z\%$) were estimated based on the transformer's nominal power rating. All transformers are configured with a Delta (Δ) connection on the primary and a Wye (Y) connection on the secondary side, with a line-to-line voltage transformation ratio of 13.8 kV/0.22 kV.

The geographical positioning of transformers is obtained using a methodology similar to that applied for the pole coordinates. Transformers are georeferenced, and the spatial distribution results are presented in Fig. 1b. A total of 96 transformers were identified, corresponding to a cumulative installed nominal power of 9,402.5 kVA. It is worth noting that this total installed capacity is significantly higher than the institution's contract demand of 2,600 kVA, indicating that the distribution system currently operates under lightly loaded conditions. This also reflects the robustness of the existing infrastructure, ensuring operational reliability and providing a substantial capacity margin to accommodate future expansions, load increases, and the integration of new technologies such as distributed generation.

D. Electrical Cable Specifications

For the medium-voltage (MV) network, conductor cross-sectional areas of 50 mm^2 and 150 mm^2 are identified, all with insulation rated for 15 kV. In the low-voltage (LV) network, conductors with cross-sectional areas of 35 mm^2, 50 mm^2, 95 mm^2, 120 mm^2, and 240 mm^2 are used. These values were collected through field inspections, while the distances between the transformer and the loads (buildings) were obtained using *Google Maps*.

E. Photovoltaic Installations

The Federal University of Lavras (UFLA) hosts several photovoltaic (PV) systems, with this study focusing on the two largest systems: *MicroPV I* and *MiniPV I*.

MicroPV I has an installed capacity of 19 kW, comprising 21 PV modules of 245 W and 250 modules of 54 W, connected to three inverters (two 5 kW and one 4 kW). It is connected to the low-voltage side of an existing 75 kVA transformer via 35 mm^2 cables. The use of a non-dedicated transformer was justified by the system's small size and proximity to the connection point. *MiniPV I* has a capacity of 1,224 kW, with 4,080 modules of 335 W distributed across 34 inverters (36 kW each), grouped into 12 solar shelters. Inverters connect to distribution panels via 16 mm^2 cables, and the outputs are linked to a dedicated 1.5 MVA step-up transformer (0.38/13.8 kV) using 120 mm^2 cables. In both systems, the geographic locations of solar shelters, inverters, panels, and transformers were determined using *Google Maps*.

F. Photovoltaic Power Generation Profile

The PV power generation profile was empirically obtained by monitoring one of the inverters at *MicroPV I*. Fig. 2 shows the normalized daily generation curve based on 15-minute interval data recorded on May 4, 2024, a day with near-nominal operating conditions and minimal cloud interference.

As the primary focus of this study is the modeling of the system and the evaluation of PV generation impacts, this generation profile is applied across all simulation scenarios, without statistical variation, representing maximum PV output and assessing system behavior under a worst-case scenario. However, it is important to highlight the relevance of incorporating statistically varied or data-driven generation profiles

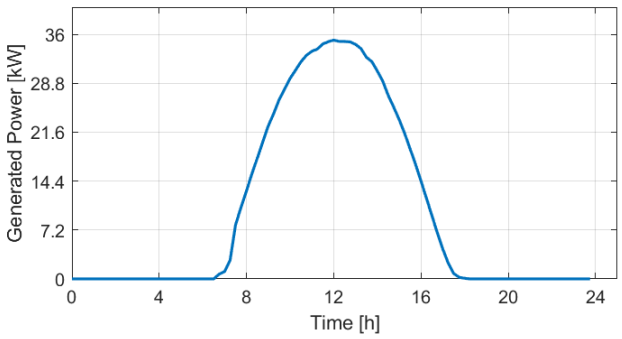

Fig. 2. Empirical generation curve of a 36 kW inverter of the *MicroPV I*.

in future studies, in order to represent different levels of solar penetration and enhance the realism of the analysis.

G. Assessment of UFLA's Load Demand Profiles

For the analysis of electrical demand curves, bulk consumption data from the main feeder were obtained from the local utility company, Companhia Energética de Minas Gerais (CEMIG), covering the period from July 1, 2022 to August 31, 2023. It is important to emphasize that this time frame was selected to ensure that the photovoltaic installation *MiniPV I* was not yet in operation, thereby representing the demand behavior without the influence of on-site generation.

During this period, the institution's academic calendar was adjusted due to the impacts of the COVID-19 pandemic. The first academic semester of 2022 took place from June 6 to September 28. The second semester began on October 24, 2022, and ended on March 23, 2023, with an end-of-year recess from December 18, 2022 to January 14, 2023. The first academic semester of 2023 was held from April 17 to August 4. These academic periods are relevant to the interpretation of the load profiles, as campus activity has a significant influence on electricity consumption.

To capture representative scenarios, eight specific weeks were selected, four academic and four vacation weeks, one from each quarter. For each quarter, the weeks with the highest and lowest recorded demands were chosen. Table I presents these periods and their respective demand values. The highest demand observed was 1,887 kVA, with a power factor of 0.92, recorded on March 1, 2023 at 3:45 PM, a Wednesday. Conversely, the lowest demand was 448 kVA (power factor of 0.64), recorded on October 16, 2022 at 9:00 AM, a Sunday.

The daily load profiles for each selected week are illustrated in Fig. 1. Figs. 3a and 3b depict a typical weekday demand pattern, with a gradual increase from 7:00 AM to 11:00 AM, a drop during the lunch break (11:00 AM–1:00 PM), and a peak between 2:00 PM and 4:00 PM. After 4:00 PM, demand decreases, with a slight rise from 6:00 PM to 9:00 PM due to

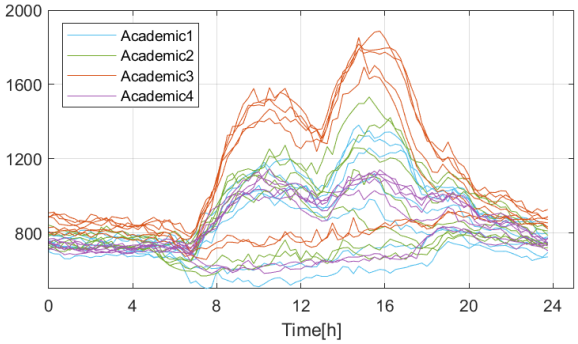

(a) Demand (kVA) - Academic Periods

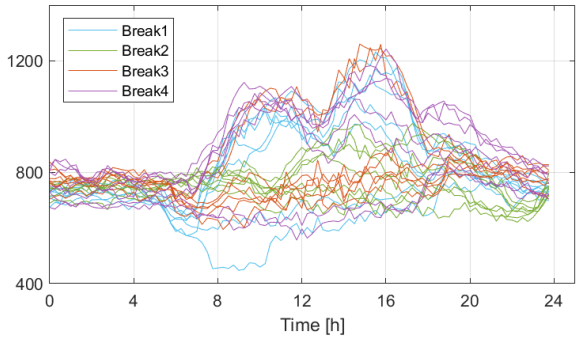

(b) Demand (kVA) - Break Periods

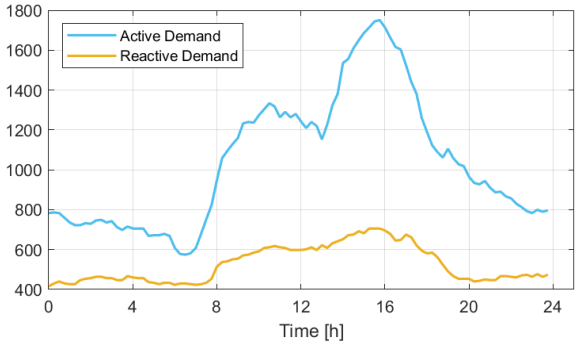

(c) Maximum Active (kW) and Reactive (kVar) Demand Profiles

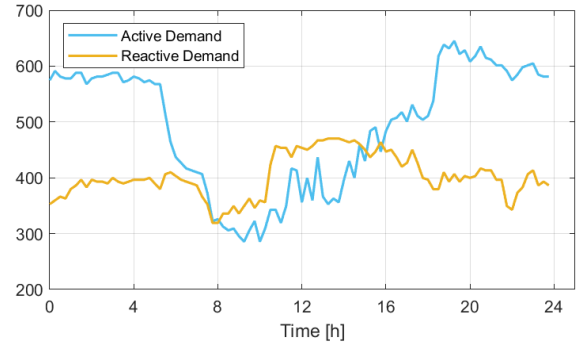

(d) Minimum Active (kW) and Reactive (kVar) Demand Profiles

Fig. 3. Apparent Power Demand Profiles [kVA] – (a) Academic Term Period, (b) Vacation Period; and Active [kW] and Reactive [kVar] Demand Profiles – (c) Day of Maximum Recorded Demand, (d) Day of Minimum Recorded Demand.

TABLE I
PERIOD OF MAXIMUM AND MINIMUM REGISTERED DEMAND

Analyzed Week	Academic Period	Demand Max.(kVA)	Demand Min.(kVA)
11–17 Sep. 2022	Academic	1382	510
16–22 Oct. 2022	Vacation	1232	**448**
20–26 Nov. 2022	Academic	1532	568
18–24 Dec. 2022	End-of-year Break	970	646
19–25 Feb. 2023	Break (Holiday)	1261	601
26 Feb.–4 Mar. 2023	Academic	**1887**	723
18–24 Jun. 2023	Academic	1146	582
16–22 Ago. 2023	Vacation	1243	556

evening academic activities. This behavior is consistent during both academic and vacation periods. On weekends, demand remains stable, with a slight daytime reduction mainly due to public lighting being switched off. This pattern is clearly observed in the active and reactive power profiles shown in Figs. 3c (March 1, Wednesday) and 3d (October 16, Sunday). It is worth noting that these load profiles reflect the specific characteristics of UFLA's consumption dynamics. These curves are used to model load behavior in daily power flow simulations, serving as a representative basis for evaluating system performance under different demand conditions.

IV. LOAD MODELING AND POWER FLOW IN OPENDSS

A. Load Allocation in Distribution Transformers

In the absence of individual load measurements for each distribution transformer, a statistical modeling approach was adopted. Rather than distributing the total demand uniformly or proportionally, a normal distribution was used to represent variability. This distribution relies on two parameters: the transformer loading (*TL*) and the system loading (*SL*).

The transformer loading of unit i (TL_i) was defined as the ratio between the apparent power consumed by the load connected to transformer i ($S_{\text{load},i}$) and its rated capacity ($S_{\text{rated},i}$). This can be expressed mathematically as:

$$TL_i\ (\%) = \frac{S_{\text{load},i}}{S_{\text{rated},i}} \times 100 \tag{1}$$

The system loading (*SL*) represents the ratio between the total apparent power demand of the entire installation ($S_{\text{load,total}}$) and the total installed rated capacity, obtained by summing the rated capacities of all N transformers in the system:

$$SL\ (\%) = \frac{S_{\text{load,total}}}{\sum_{i=1}^{N} S_{\text{rated},i}} \times 100 \tag{2}$$

In the analyzed system, the total installed transformer capacity is 9,402.5 kVA. Over the observation period, the maximum recorded demand was 1,887 kVA, corresponding to a system loading of $SL = 20.07\%$. The minimum demand recorded was 447.57 kVA, resulting in $SL = 4.76\%$.

To model the variability of transformer loading across the network, it is assumed that each TL_i follows a normal distribution centered on the average system loading (*SL*), with a predefined standard deviation σ. This assumption captures the heterogeneous energy consumption profiles found across campus facilities. For instance, on weekdays, significant variation is expected among departments, laboratories, and classrooms. Conversely, on weekends, when only essential systems are active, transformer loading tends to be more homogeneous.

Under the assumption that all the transformer loadings (TL_i) follow a normal distribution, most values are expected to fall within three standard deviations of the mean, as:

$$SL - 3\sigma < TL_i < SL + 3\sigma \tag{3}$$

The standard deviation σ is selected for each scenario to ensure that all TL_i values remain within realistic operational boundaries and do not take negative values. For instance, when $SL = 20.07\%$, choosing $\sigma = 6.7\%$ guarantees that all transformer loadings remain below 50%. Similarly, in the low-demand scenario where $SL = 4.76\%$, a standard deviation of $\sigma = 1.58\%$ keeps all TL_i values below 15%.

Likewise, power factor values were assigned based on the same statistical methodology, ensuring their distribution remains within physically meaningful limits, i.e., between 0 and 1.

B. Simulation Studies in OpenDSS

Taking these assumptions into account, four load distribution scenarios were defined for the power flow studies, described as follows:

- **Scenario A:** Loads is distributed among the transformers with an average loading (*GL*) of 4.76%, indicating the minimum recorded demand, and a σ of 1.58%. The average power factor (FP_m) is 0.64, with a σ of 0.12;
- **Scenario B:** Loads is distributed among the transformers with an *GL* of 20.06%, corresponding to the maximum recorded demand, and a σ of 6.69%. The FP_m is set to 0.92, with a σ of 0.03;
- **Scenario C:** OpenDSS performs a daily simulation, with the loads from Scenario A adjusted to follow the profile illustrated in Fig. 3d, representing the day with the minimum recorded demand;
- **Scenario D:** OpenDSS performs a daily simulation, with the loads from Scenario B adjusted to follow the profile illustrated in Fig. 3c, representing the day with the maximum recorded demand.

The proposed scenarios enable deterministic evaluation of the distribution system's behavior under both low and high demand conditions. Scenarios C and D allow time-series analysis over 24 hours, providing a more comprehensive assessment of system dynamics throughout the day. These scenarios are first evaluated without the integration of the photovoltaic plants MiniPV I and MicroPV I. Subsequently, the impact of these distributed generators is assessed, followed by a final analysis that incorporates reactive power compensation.

C. Capacitor Bank Sizing Procedure

To enhance the power factor at the feeder, an iterative search-based approach is adopted. The search strategy consists of a deterministic incremental method, in which a fixed unit of 100 kVAr of capacitive compensation is added at a single-point location, uniquely allocated at the feeder. After each addition, Power flow analysis is performed in OpenDSS via Python,

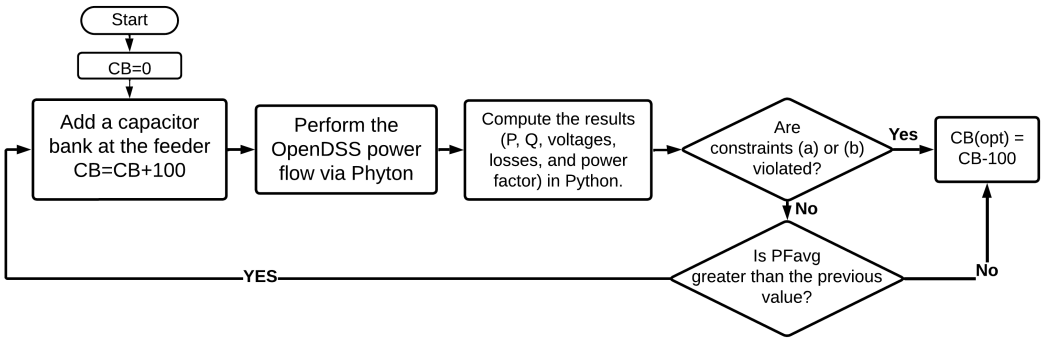

Fig. 4. Flowchart of the Capacitor Bank Sizing Algorithm.

and the results are verified within Python to ensure that all operational constraints are satisfied.

The objective is to maximize the average daily power factor measured at the feeder. The objective function is defined as:

$$\max \ PF_{\text{avg}} = \frac{1}{T}\sum_{t=1}^{T} PF(t) \tag{4}$$

where, PF_{avg} denotes the average power factor in the feeder over the course of the day. The variable $PF(t)$ represents the instantaneous power factor at time step t, and T corresponds to the total number of time steps considered in the analysis period.

The optimization is subject to the following constraints:

(a) **Voltage limits**: all nodal voltages V_i must remain within regulatory bounds, that is, 0.95 p.u. $< V_i(t) < 1.05$ p.u. for all i and all t.

(b) **No overcompensation**: the total capacitive compensation Q_c must not exceed the total reactive power demand of the system at any time, i.e., $Q_c \leq Q(t)$.

The stopping criteria of the algorithm are defined as follows: if either condition (a) or (b) is violated at any iteration, the algorithm terminates, and the optimal capacitor bank size is set to the last feasible value. If both conditions are satisfied, the algorithm checks whether the average power factor has improved relative to the previous iteration. If so, the algorithm proceeds to the next iteration; otherwise, it stops, and the optimal capacitor bank size is set to the last feasible value. The algorithm is illustrated by the flowchart shown in Fig. 4.

The proposed capacitor bank sizing algorithm is implemented through a Python script using the native OpenDSSDirect interface. This automation allows the execution of power flow simulations directly in OpenDSS while controlling the iterative incremental addition of capacitor units and verifying the system operational constraints in Python.

However, some aspects were not considered, such as the variability of photovoltaic generation due to environmental conditions (e.g., temperature, efficiency, and shading), and the use of switched capacitor banks. Although switched banks would better accommodate the significant fluctuations in demand observed at the Federal University of Lavras (UFLA), especially between academic and vacation periods, the proposed analysis adopts fixed banks applied separately in the minimum and maximum demand scenarios (Scenarios C and D), allowing the determination of lower and upper compensation limits.

V. Results

This section presents the results obtained through power flow simulations performed in *OpenDSS*, including both deterministic and time-series (daily) analyses.

A. Deterministic Power Flow Analysis

The results of the power flow simulations performed in OpenDSS for the minimum demand condition (Scenario A) and the maximum demand condition (Scenario B), both evaluated with and without the integration of Distributed Generation (DG), are presented in Fig. 5 and Table II.

For Scenario A (Figs. 5a, 5b and Table II), the integration of DG results in net negative active power of -950.03 kW, indicating energy export to the grid. Active power losses increase from 0.47 kW to 18.93 kW, and line reactive power consumption rises from 1.14 kVar to 67.22 kVar, mainly due to elevated current in segments with smaller cross-section cables. The power factor improves from 0.64 to 0.92, as the injected active power exceeds the original demand (273.97 kW), while reactive power remains nearly unchanged. The maximum voltage increases by approximately 2%. The voltage range stays within regulatory limits, varying from 0.99 pu to 1.01 pu, in compliance with PRODIST — Module 8 [21].

In Scenario B (Figs. 5c, 5d and Table II), DG reduces active power demand from $1{,}703.35$ kW to 474.18 kW. However, losses increase: active losses rise from 9.13 kW to 22.81 kW, and line reactive power consumption grows from 21.29 kvar to 85.13 kvar, mainly due to power flow redistribution. The power factor drops from 0.92 to 0.51, as active demand decreases significantly while reactive power remains nearly unchanged. A 2% rise in maximum voltage is also observed, with voltages ranging from 0.97 pu to 1.01 pu, remaining within the limits specified in PRODIST — Module 8 [21].

In general, the results show that integrating DG units into the UFLA EDS shifts the power flow pattern from a predominantly centralized supply at the main feeder to more localized flows near the generation units, as expected. This redistribution, combined with the specific characteristics of

the network near the DG units, leads to increased active and line reactive power consumption under both minimum and maximum demand conditions.

B. Daily Power Flow Analysis

The daily power flow analysis enables a detailed evaluation of the system's dynamic behavior under typical load and generation conditions. Figs. 6a, 6b, 6c, and 6d present the results for Scenario C. In Fig. 6a, the active power curve shows a reversal in flow direction during most daylight hours due to DG integration, as previously observed in the deterministic analysis. Fig. 6b indicates a slight increase in reactive power following DG integration, mainly due to increased current flow and associated line (cables) losses. Fig. 6c shows that the power factor becomes highly sensitive to active power fluctuations. However, even before DG integration, the power factor was already below the regulatory threshold of 0.92 [21].

To mitigate this, a 400 kVar fixed capacitor bank was allocated using the optimization procedure described in Section IV-C. As seen in Fig. 6b, this addition was effective in reactive power compensation during nighttime and significantly reduced daytime consumption, resulting in an overall improvement in power factor. Despite the voltage rise caused by the capacitor bank, shown in Fig. 6d, voltage levels remained within acceptable operational limits.

Figs. 6e, 6f, 6g, and 6h present the corresponding results for Scenario D (high load condition). In Fig. 6e, most of the active power generated by DG is consumed locally, with minimal export to the grid. Fig. 6f again shows a slight increase in reactive power due to DG insertion. Fig. 6g reveals that the power factor remains highly sensitive to the balance between generation and load, reaching very low values when the net active power at the feeder approaches zero, a condition that is particularly difficult to regulate. A 400 kVar capacitor bank was also allocated in this scenario. As shown in Fig. 6h, the bank improved nighttime power factor and slightly mitigated daytime deviations. Voltage levels show a small increase but remained well below regulatory thresholds.

The capacitor bank improved both voltage profiles and power factor in Scenarios C and D. However, the variability of load and generation poses challenges for effective compensation using fixed reactive resources alone. Therefore, more flexible solutions, such as switched capacitor banks, adaptive control strategies, or inverter-based reactive control may be necessary in future studies to achieve more robust compensation across varying operating conditions. Moreover, no voltage violations were observed in any scenario, even with DG and reactive compensation. To ensure local overvoltages did not occur in secondary circuits, voltage levels were monitored at the secondary circuits, all remaining below 1.03 pu.

It is also worth noticing that the same PV generation profile was used across all scenarios, without statistical variation or intermediate generation levels. Nevertheless, it is understood that maximum and minimum generation scenarios would produce results between the upper and lower bounds already captured in the current simulations, effectively covering the expected operational envelope for active/reactive power and voltage behavior.

VI. Conclusion

This paper presented a practical methodology for modeling real Electrical Distribution Systems (EDSs) directly in OpenDSS, without relying on georeferenced datasets or commercial GIS tools. Satellite imagery was employed to identify network components, significantly reducing fieldwork, while complementary technical data were obtained via targeted inspections. Load allocation combined measurements and statistical techniques to capture demand variability, enabling a simulation framework that includes primary and secondary networks, as well as existing PV systems. Simulations revealed that DER integration alters power flow patterns, increases losses, and impacts voltage profiles and power factor, particularly during peak demand.

To adjust power factor, a simple deterministic incremental algorithm was proposed to determine the optimal size of a fixed capacitor bank installed at the feeder. Despite its simplicity, the algorithm effectively improved the average daily power factor and ensured compliance with operational constraints. Its main benefits include ease of implementation, transparency, and suitability for preliminary planning studies.

The proposed methodology achieved its objective of accurate modeling and analysis of a real-world EDS via a simplified and accessible process. Nonetheless, some limitations remain, including the absence of advanced load disaggregation, statistical analysis of the PV profile, real-time monitoring data, and the application of optimization techniques. Future work could address these aspects by integrating switched capacitor banks, inverter-based control strategies, and smart meter data to enhance modeling accuracy and operational flexibility.

TABLE II
POWER FLOW RESULTS UNDER MINIMUM AND MAXIMUM DEMAND CONDITIONS, WITH AND WITHOUT DISTRIBUTED GENERATION (DG)

	Scenario A		Scenario B	
Description	**Without DG**	**With DG**	**Without DG**	**With DG**
Total Installed DG (kW)	–	1243	–	1243
Maximum Voltage (p.u.)	0.99	1.02	0.99	1.01
Minimum Voltage (p.u.)	0.99	1.00	0.97	0.97
Total Active Power (kW)	274.22	–950.03	1703.35	474.18
Total Reactive Power (kVar)	326.98	393.06	715.13	778.96
Power Factor	0.64	–0.92	0.92	0.51
Line Active Power Losses (kW)	0.47 (0.17%)	18.93 (–1.99%)	9.13 (0.53%)	22.81 (4.81%)
Line Reactive Power Consumption (kVar)	1.14 (0.34%)	67.22 (17.10%)	21.29 (2.97%)	85.13 (10.92%)

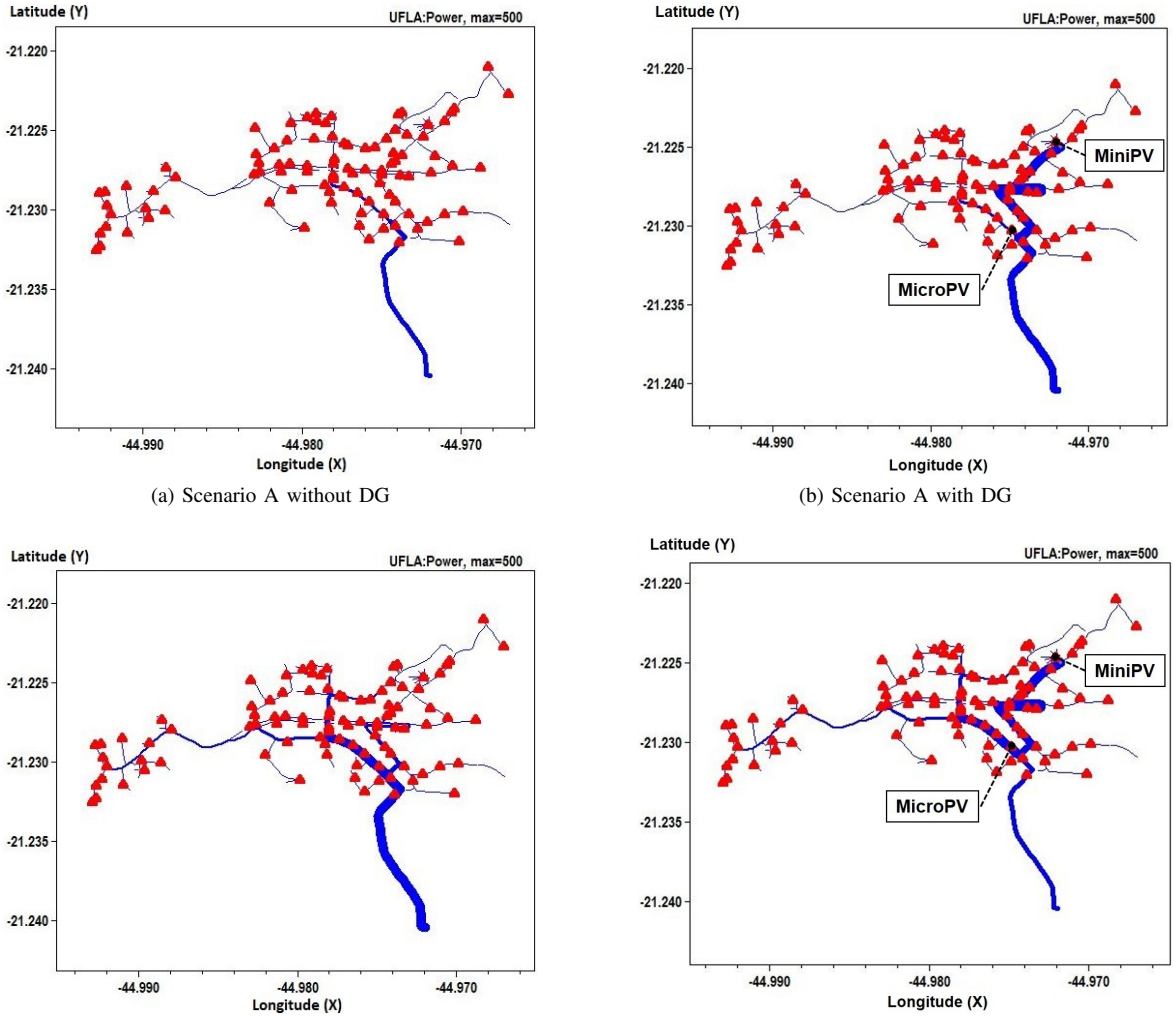

(a) Scenario A without DG

(b) Scenario A with DG

(c) Scenario B without DG

(d) Scenario B with DG

Fig. 5. Power flow analysis in OpenDSS for: (a) Scenario A without DG, (b) Scenario A with DG, (c) Scenario B without DG, and (d) Scenario B with DG.

ACKNOWLEDGMENTS

The authors thank FAPEMIG, CNPq and CAPES for financial support, and UFLA for providing technical data and infrastructure essential to this work.

REFERENCES

[1] D. K. Mishra, M. J. Ghadi, A. Azizivahed, L. Li, and J. Zhang, "A review on resilience studies in active distribution systems," *Renewable and Sustainable Energy Reviews*, vol. 135, p. 110201, 2021. doi:10.1016/j.rser.2020.110201.

[2] J. M. Home-Ortiz, O. D. Melgar-Dominguez, M. S. Javadi, J. R. S. Mantovani, and J. P. S. Catalão, "Improvement of the distribution systems resilience via operational resources and demand response," *IEEE Transactions on Industry Applications*, vol. 58, no. 5, pp. 5966–5976, 2022. doi:10.1109/TIA.2022.3190241.

[3] R. Zubo, G. Mokryani, H.-S. Rajamani, J. Aghaei, T. Niknam, and P. Pillai, "Operation and planning of distribution networks with integration of renewable distributed generators considering uncertainties: A review," *Renewable and Sustainable Energy Reviews*, vol. 72, pp. 1177–1198, 2017. doi:10.1016/j.rser.2016.10.036.

[4] R. Dashti and M. Rouhandeh, "Power distribution system planning framework (a comprehensive review)," *Energy Strategy Reviews*, vol. 50, p. 101256, 2023. doi:10.1016/j.esr.2023.101256.

[5] M. Mahdavi and R. Romero, "Reconfiguration of radial distribution systems: An efficient mathematical model," *JIEEE Latin America Transactions*, vol. 19, no. 7, pp. 1172–1181, 2021. doi:10.1109/TLA.2021.9461846.

[6] V. de Cillo Moro, R. S. Bonadia, and F. C. L. Trindade, "A review of methods for assessing der hosting capacity of power distribution systems," *JIEEE Latin America Transactions*, vol. 20, no. 10, pp. 2275–2287, 2022. doi:10.1109/TLA.2022.9885165.

[7] R. C. de Oliveira, S. C. Ferreira, and B. H. D. Kai, "Capacidade de hospedagem de sistemas fotovoltaicos em redes de distribuição," *IX Brazilian Symposium on Electrical Systems - SBSE*, vol. 2, no. 1, 2022. doi:10.20906/sbse.v2i1.3042.

[8] E. Mulenga, M. H. Bollen, and N. Etherden, "A review of hosting capacity quantification methods for photovoltaics in low-voltage distribution grids," *International Journal of Electrical Power and Energy Systems*, vol. 115, p. 105445, 2020. doi:10.1016/j.ijepes.2019.105445.

[9] J. Tello-Maita, A. Marulanda, and A. Pavas, "Simulation of modern distribution systems using matlab and opendss," in *2019 FISE-IEEE/CIGRE Conference - Living the energy Transition (FISE/CIGRE)*, pp. 1–6, 2019. doi:10.1109/FISECIGRE48012.2019.8984949.

[10] G. Gonzalo, A. Aguila, D. Gonzalez, and L. Ortiz, "Optimum location and sizing of capacitor banks using volt var compensation in microgrids," *JIEEE Latin America Transactions*, vol. 18, no. 3, pp. 465–472, 2020. doi:10.1109/TLA.2020.9082717.

[11] R. Gautam, S. Khadka, T. B. Malla, A. Bhattarai, A. Shrestha, and F. Gonzalez-Longatt, "Assessing uncertainty in the optimal

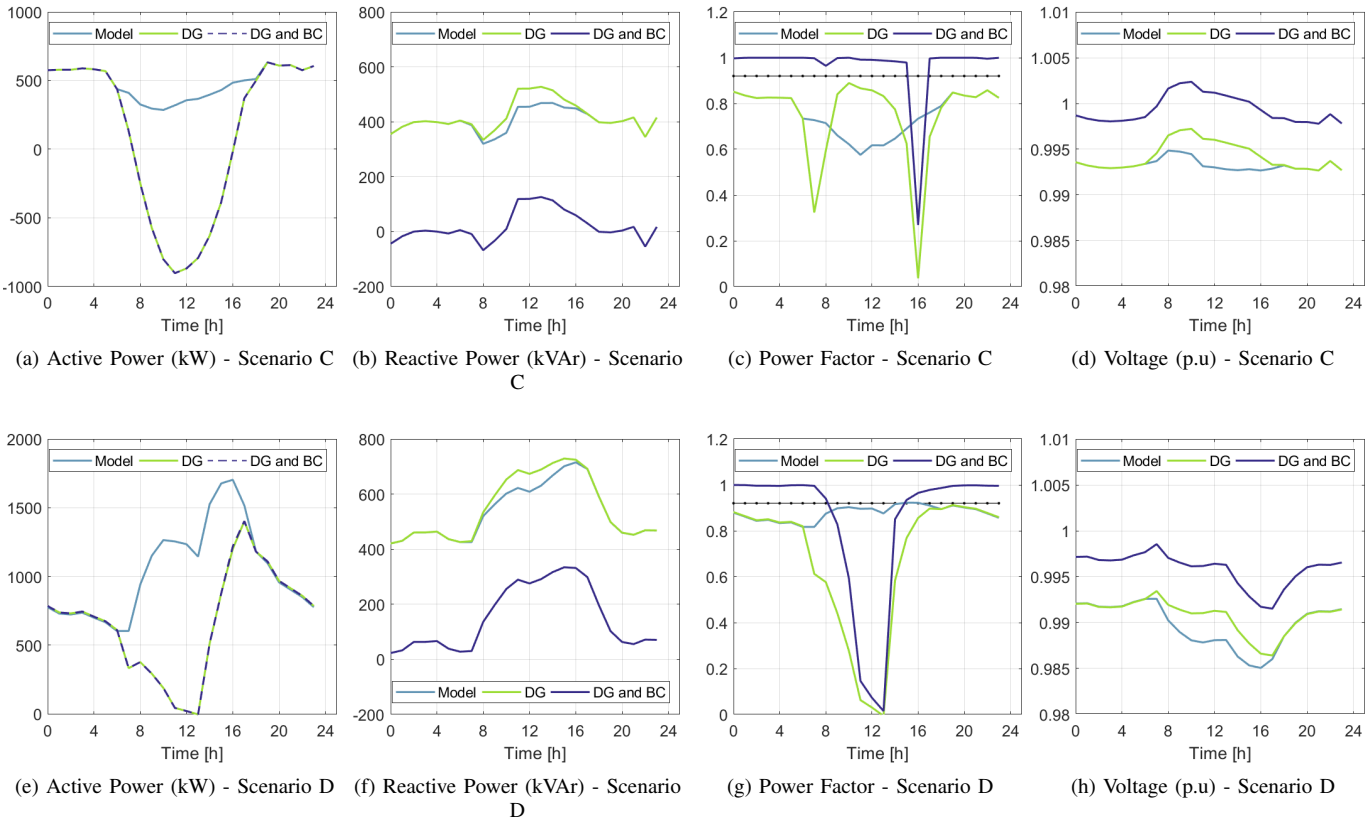

(a) Active Power (kW) - Scenario C (b) Reactive Power (kVAr) - Scenario C (c) Power Factor - Scenario C (d) Voltage (p.u) - Scenario C

(e) Active Power (kW) - Scenario D (f) Reactive Power (kVAr) - Scenario D (g) Power Factor - Scenario D (h) Voltage (p.u) - Scenario D

Fig. 6. Daily profile for Scenario C — (a), (b), (c), (d) and Scenario D — (e), (f), (g), (h) under three distinct operating conditions: without distributed generation (Model), with distributed generation (DG), and with distributed generation and capacitor bank (DG and BC).

placement of distributed generators in radial distribution feeders," *Electric Power Systems Research*, vol. 230, p. 110249, 2024. doi:10.1016/j.epsr.2024.110249.

[12] L. R. Braz Pontes, Y. Percy Molina Rodriguez, J. Luyo Kuong, and H. Rojas Espinoza, "Optimal allocation of energy storage system in distribution systems with intermittent renewable energy," *JIEEE Latin America Transactions*, vol. 19, no. 2, pp. 288–296, 2021. doi:10.1109/TLA.2021.9443071.

[13] F. Ahmad, A. Iqbal, I. Ashraf, M. Marzband, and I. khan, "Optimal location of electric vehicle charging station and its impact on distribution network: A review," *Energy Reports*, vol. 8, pp. 2314–2333, 2022. doi:10.1016/j.egyr.2022.01.180.

[14] U. H. Ramadhani, M. Shepero, J. Munkhammar, J. Widén, and N. Etherden, "Review of probabilistic load flow approaches for power distribution systems with photovoltaic generation and electric vehicle charging," *International Journal of Electrical Power and Energy Systems*, vol. 120, p. 106003, 2020. doi: 10.1016/j.ijepes.2020.106003.

[15] K. Montano-Martinez, S. Thakar, S. Ma, Z. Soltani, V. Vittal, M. Khorsand, R. Ayyanar, and C. Rojas, "Detailed primary and secondary distribution system model enhancement using ami data," *IEEE Open Access Journal of Power and Energy*, vol. 9, pp. 2–15, 2022. doi: 10.1109/OAJPE.2021.3125900.

[16] X. Zhu, M. Emmanuel, G. Julieta, I. Krad, W. Wang, B. Palmintier, W.-H. Chen, A. Hirayama, and M. Asano, "Real-world distribution system modeling framework for transmission-and-distribution cosimulation," in *2020 47th IEEE Photovoltaic Specialists Conference (PVSC)*, pp. 1575–1580, 2020. doi:10.1109/PVSC45281.2020.9300406.

[17] R. E. De-Jesús-Grullón, R. O. Batista Jorge, A. Espinal Serrata, J. E. Bueno Díaz, J. J. Pichardo Estévez, and N. F. Guerrero-Rodríguez, "Modeling and simulation of distribution networks with high renewable penetration in open-source software: Qgis and opendss," *Energies*, vol. 17, no. 12, 2024. doi:10.3390/en17122925.

[18] K. Montano-Martinez, S. Thakar, V. Vittal, R. Ayyanar, and C. Rojas, "Detailed primary and secondary distribution system feeder modeling based on ami data," in *2020 52nd North American Power Symposium (NAPS)*, pp. 1–6, 2021. doi: 10.1109/NAPS50074.2021.9449779.

[19] S. S. Saha, K. Montano-Martinez, J. Peppanen, M. Rylander, and L. O'Mahony, "Geolocating on-ground distribution system assets using ami data," in *2023 IEEE Power and Energy Society General Meeting (PESGM)*, pp. 1–5, 2023. doi: 10.1109/PESGM52003.2023.10252225.

[20] Google, "Ufla electrical distribution system map." https://www.google.com/maps/d/u/0/edit?mid=1TxKzTqwEfGx__l0Tg8phycSTLsyf0gA&usp=sharing, 2025. Accessed: Jun. 06, 2025.

[21] Agência Nacional de Energia Elétrica (ANEEL), "PRODIST - Módulo 8: Qualidade da Energia Elétrica, versão 11," 2020. Available at: https://www2.aneel.gov.br.

Sílvia Costa Ferreira received her B.Sc. (2010), M.Sc. (2012), and Ph.D. (2016) degrees in Electrical Engineering from the Federal University of Itajubá (UNIFEI), Brazil. She is currently a Professor at the Federal University of Lavras (UFLA), Brazil. Her research interests are focused on Electrical Engineering, with particular emphasis on Industrial Electronics and Automation, encompassing power electronics, distributed generation systems, microgrids, control systems, and electrical power systems.

Ronnielli Chagas de Oliveira received his B.Sc. in Electronic and Telecommunications Engineering from Pontifical Catholic University of Minas Gerais (2016) and the M.Sc. in Systems and Automation Engineering from UFLA (2021). He has worked as a technical instructor at CEFET-MG and other Anima Group institutions, also delivering professional training on distributed generation systems. Currently, he works in distributed generation and microgrids.

Alexandre de Araújo received his B.Sc. in Control and Automation Engineering from Faculdade Anhanguera de Jacareí (2018) and the M.Sc. in Systems and Automation Engineering from UFLA (2024). He is pursuing a Ph.D. in Telecommunications at INATEL. His professional activities include electrical project design, distributed generation, industrial automation, and project management in the electrical sector.

Alexandre Luiz da Silva received his B.Sc. in Electrical Engineering from CEFET-MG, Nepomuceno Campus (2021). He is currently pursuing a master's degree in Systems and Automation Engineering at UFLA. At UFLA, he works as an Electromechanical Technician in the Engineering Department. Concurrently, he is involved in electrical project development, distributed generation systems, and serves as a co-owner of a solar energy company.

Marcelo Arriel Rezende received his B.Sc. in Industrial Electrical Engineering from the Federal University of São João del Rei (2007) and a specialization in Occupational Safety Engineering from the University of Campinas (2010). He is an Electrical Engineer at UFLA and has extensive experience in industrial, building, and power distribution electrical projects. His expertise includes industrial and building electrical projects, medium and low-voltage distribution, and distributed energy systems.

João Paulo de Carvalho Pedroso received his B.Sc. (2015) in Water Resources Engineering from the Federal University of Itajubá and the M.Sc. (2022) in Systems and Automation Engineering from UFLA, Brazil. He received the Ph.D. (2025) in Agricultural Engineering from UFLA and served as a Visiting Researcher (2023–2024) at the Center for Research on Microgrids (CROM), Aalborg University, Denmark. His research interests include microgrids, energy management, multi-objective optimization, and renewable energy systems.

Joaquim Paulo da Silva received his B.Sc. degree in Industrial Electrical Engineering from the Federal University of São João Del-Rei (1988), the M.Sc. degree in Electrical Engineering from the Federal University of Itajubá (1993), and the Ph.D. degree in Electrical Engineering from the Federal University of Minas Gerais (2001). He is currently a Full Professor at the Federal University of Lavras, where his research focuses on photovoltaic and wind renewable energies, energy efficiency, and innovation in new materials.